Up-cycling waste glass to minimal water adsorption / absorption lightweight aggregate by rapid low temperature sintering: optimization by dual process-mixture response surface methodology

Costas A. Velis[a, b,*] *Claudia Franco-Salinas*[a], *Catherine O'Sullivan*[a], *Jens Najorka*[c], *Aldo R. Boccaccini*[d], *Christopher R. Cheeseman*[a, *]

[a] Department of Civil and Environmental Engineering, Imperial College London, South Kensington Campus, London SW7 2AZ, UK

[b] School of Civil Engineering, University of Leeds, Leeds LS2 9JT, UK

[c] Department of Mineralogy, The Natural History Museum, Cromwell Road, London SW7 5BD, UK

[d] Institute of Biomaterials, Department of Materials Science and Engineering, University of Erlangen-Nuremberg, Cauerstr. 6, 91058 Erlangen, Germany

* Corresponding authors: (1) *Christopher R. Cheeseman:* Tel.: + 44 (0) 207 594 5971

e-mail: c.cheeseman@imperial.ac.uk

(2) *Costas A. Velis:* Tel.: + 44 (0) 113 343 2327

e-mail: c.velis@leeds.ac.uk

Abstract. Mixed colour waste glass extracted from municipal solid waste is either not recycled, in which case it is an environmental and financial liability, or it is used in relatively low value applications such as normal weight aggregate. Here, we report on converting it into a novel glass-ceramic lightweight aggregate (LWA), potentially suitable for high added value applications in structural concrete (upcycling). The artificial LWA particles were formed by rapidly sintering (<10 min) waste glass powder with clay mixes using sodium silicate as binder and borate salt as flux. Composition and processing were optimised using response surface methodology (RSM) modelling, and specifically: (i) a combined process-mixture dual RSM, and (ii) multi-objective optimisation functions. The optimisation considered raw materials and energy costs. Mineralogical and physical transformations occur during sintering and a cellular vesicular glass-ceramic composite microstructure is formed, with strong correlations existing between bloating / shrinkage during sintering, density and water adsorption / absorption. The diametrical expansion could be effectively modelled via the RSM and controlled to meet a wide range of specifications; here we optimised for LWA structural concrete. The optimally designed LWA is sintered in comparatively low temperatures (825-835 °C), thus potentially saving costs and lowering emissions; it had exceptionally low water adsorption / absorption (6.1-7.2% w/w_d; optimisation target: 1.5-7.5% w/w_d); while remaining substantially lightweight (density: 1.24-1.28 $g.cm^{-3}$; target: 0.9-1.3 $g.cm^{-3}$). This is a considerable advancement for designing effective environmentally friendly lightweight concrete constructions, and boosting resource efficiency of waste glass flows.

Keywords: Waste glass; Lightweight aggregate; Resource efficiency; Solid waste management, Resource efficiency, Up-cycling; Response surface methodology; Borates

1. Introduction

Maximising the value we can extract from waste and treating them as flows of 'technical nutrients' and up-cycling them (improving their value via recycling), could be a critical factor in managing resources to secure a sustainable future.[1] Key to success is a combination of innovative materials processing, as new ideas[2, 3] in this research area demonstrate, combined with the application of advanced environmental and materials engineering tools, such as response surface methodology (RSM),[4, 5] to waste and secondary raw material reprocessing. Recovering value from waste glass is a major challenge: issues concerned with collection, colour and type separation still limit recycling (e.g. mixing of pyroceramic, lead-crystal, ovenware type, and drinking glasses with soda-lime-silicate glasses).[6] For example, material flow analysis demonstrated that for waste glass stemming from consumer beverages in New Jersey in 2008, only a small amount (about 11% wt.) was used for glass manufacturing, the bulk of it being used as construction aggregate – a low value (open-loop or downcycling) and wasting energy application.[7] The challenge is particularly pertinent for the mixed colour glass cullet smaller than 10 mm, such as often encountered in the reject fractions of mechanical-biological treatment (MBT) plants[8] and material recycling facilities (MRF) processing municipal solid waste. For such finely sized and contaminated streams optical sorting is unable to render sufficient recovery results and residues are often disposed of in landfills rather than being beneficially utilised. Disposal or use as low value aggregate wastes significant embodied energy and materials contained in the glass along with opportunities for material substitution[7], which even in cases of thermal reprocessing have been shown to avoid hundreds kg CO_2-eq. per tonne of glass waste.[9] The development of new recycling options, particularly for problematic mixed colour glass, is therefore required to increase its beneficial post-consumption fate.[10] As a result, there is on-going research and innovation in this wider

area (indicatively: use of soda-lime-silica glass as feedstock for the production of tobermorite)[11].

At the same time, there is increasing demand for ceramic lightweight aggregate (LWA) particles with densities significantly less than 1.60 g.cm^{-3} for use in light aggregate concrete (LWAC). Pre-cast LWAC components are a key development in sustainable, environmentally friendly construction, and their use is increasing with the application of LWA such as Lytag.[12] LWAC offers the technical advantages of easier handling and reduced construction times, while enabling the manufacturing of larger components off-site with suitable quality control in place. Transport costs for pre-cast LWAC are also significantly reduced compared to normal weight concrete and so are transport-related air emissions due to lower weight. As a result, the development of artificial LWA particles engineered to the required combination of properties is an important research area.[13, 14]

A range of waste materials have previously been investigated for the production of artificial LWA.[14-17] A major technical disadvantage of commercially available artificial LWAs is their high water absorption which can result in different interfacial transition zone with the cement paste,[18] increase the possibility of surface cracking of the concrete or decrease its strength,[13] and cause heterogeneity in the paste, leading to low concrete stability, high permeability and low workability.[13, 19] Commercial and logistics issues are also related to the need for pre-wetting of highly absorbent LWAs. Thus, it would be highly beneficial if an artificial LWA for structural precast concrete applications could be engineered to absorb considerably less water before (pre-wetting) or during contact with the cement paste. Another key limitation of commercially available artificial LWAs is the high temperature needed during manufacturing (e.g. 1400 °C);[12] a much lower sintering temperature could bring significant energy, emissions and cost savings, delivering sustainability benefits. Additional

benefits can stem from material substitution, by avoiding pumice extraction, and transport emissions, especially for areas that have to import it from afar.

The research reported here uses the lowest quality of waste glass cullet, i.e., the most difficult to be recycled, as the main secondary raw material to manufacture an added value product (up-cycling). The use of waste glass, clay, sodium silicate and an expansive agent to form LWA has previously been reported.[20, 21] LWA has also been produced by combining lignite coal fly ash and recycled glass.[22] The addition of waste glass provided an amorphous phase which reduced the water absorption of LWA prepared from clay and sewage sludge.[23] The properties of LWAC containing expanded glass LWA have also been reported.[24]

Here we aim to develop a sustainable LWA for use in precast LWAC structural components. The novel LWA is produced by rapid thermal processing (sintering) of waste glass, clay, sodium silicate, borate materials mixture at relatively low temperatures; borate salts are added as a flux to lower the melting point and reduce melt viscosity.[25-27] We aim to engineering a LWA with minimal water absorption.

RSM is a statistical design of experiments methodology, increasingly used to develop and optimise products and model processes within the environmental sciences and engineering.[4, 5] It has not previously been used for LWA production. RSM is particularly useful when properties depend on variables such as composition and sintering temperature, for which the underlying physical mechanisms are unclear, and where complex non-linear interdependencies exist. I addition, dual RSM can produce a statistically validated predictive empirical model able to optimise both the average (target) values and the variability.[28] Concurrent multiple factor optimisation is applied here, benefiting from advances in desirability optimisation methodology (DOM).[29]

These methods are used here to develop a formulation and rapid sintering procedure to manufacture novel LWA products to exact and advanced specifications (low water absorption

and low sintering temperature). The optimal LWA is characterised to validate the optimisation outcome, and mineralogy, microstructure and strength aspects are examined.

2. Experimental

2.1. Materials

Mixed colour glass cullet (Stacey, UK) was received as a fine dry powder, with a median particle size of 65 µm and 90% vol. less than 114 µm. There was no significant paper fibre contamination in the milled glass. Donnington fireclay (Castle Claysales Ltd., UK) was supplied as a homogeneous fine powder. The chemical composition, moisture content and loss on ignition of the as-received glass and clay are given in supporting information (SI) Table S1.

Sodium pentaborate decahydrate ($Na_2O{\cdot}5B_2O_3{\cdot}10H_2O$, Polybor Flow®, Rio Tinto Borax, UK) was used as an aqueous stable suspension of sodium borate with an active boric oxide (B_2O_3) content of 32.2-33.5% wt. This was diluted 5:1 v/v using tap water before use. Sodium silicate solution (Crystal 0075, PQ Corporation, UK) with a total Na_2O content of 8.4-8.8% wt. and a SiO_2:Na_2O ratio of 3.15-3.25:1 was used to increase the unfired (i.e., green) strength of LWA pellets.

2.2. Lightweight aggregate manufacturing

Preliminary experiments identified an initial composition range and key processing factors for further investigation. Dry glass cullet powder and fireclay were mixed for 2 minutes. Tap water, sodium silicate solution and dilute sodium pentaborate decahydrate were then added to form a paste that could be hand-rolled into roughly spherical pellets (Ø=10-14 mm). The green pellets were coated with a thin layer of calcium carbonate powder (99+%, reagent grade, Aldrich, UK) to inhibit pellet bonding during sintering.

The thermal processing cycle involved pre-drying, rapid heating and rapid cooling. Pre-drying for 24 hours at 40±2 °C reduced the pellet moisture content and resulted in less variable LWA properties. Dried pellets were rapidly sintered for 20.0 ± 0.1 minutes by placing samples directly into a furnace (Lenton UK, EFC 11/8 chamber furnace) pre-heated to specified temperatures between 750 and 900 °C. Heat treating above 900 °C caused excessive bloating. Immediately after the sintering holding time, the pellets were removed from the furnace and rapidly air cooled, with ambient temperatures (ca 20±5 °C) reached in less than 5 mins. This decision prevented potential further uncontrolled volumetric changes that could have occurred during slow cooling because of: (1) ongoing irregular foaming of a partially solidified hot pellet; and (2) undesirable large-scale formation of crystalline phases which could contribute to sudden volume changes due to phase transitions (quartz 573ºC and cristobalite ~250ºC).

2.3. Raw materials and lightweight aggregate characterisation

The crystalline phases present in raw materials and fired LWA pellets were determined by X-ray diffraction (XRD, Nonius PDS120 Powder Diffraction System). XRD combined a Cobalt source, a primary Ge (111) monochromator and an INEL 120º curved position sensitive detector. The samples were measured in flat-plate asymmetric reflection geometry with tube operating conditions of 35 KV and 30 mA. Phase identification was performed with the X'Pert HighScore Plus software in conjunction with the powder diffraction file (PDF) database from the International Centre for Diffraction Data (ICDD).

The particle density of oven-dried LWA (ρ_{rd}) and the 24-hour water absorption (WA_{24}) were determined simultaneously using Archimedes' liquid displacement principle as specified in BS EN 1097-6: 2000.[30] The method was modified by using the vacuum method described for ceramic tiles in BS EN ISO 10545-3:1997.[31] Air was removed from connected

porosity, so that maximum impregnation of the intrusion medium occurred, in this case vacuum-degassed tap water. LWA pellets were held under vacuum for 1 hour before being immersed under 10 ± 1 cm of vacuum-degassed tap water at 21 ± 0.5 °C for 24 hours. Despite that the tests and established terminology refer to water "absorption", it can be reasonably assumed that this measurement includes also water adsorbed on the LWA pellet. However, standard terminology is followed onwards.

A bloating index was calculated as the relative diametrical expansion percentage ($\%\Delta D_{bl}$) of the pellet diameter before (D_i) and after (D_f) rapid firing (Appendix, Eq. A1). The moisture content (M) (w/w_d) of raw materials was measured by oven drying at 105-110 °C for 24 hours.

The indirect tensile strength of LWA pellets was determined.[32] The secant stiffness and the mass-specific energy to fracture were measured using individual pellet compression test equipment.[33] The secant stiffness K (N mm^{-1}) was calculated by dividing the failure load by the total particle linear deformation, i.e. as the slope of a line connecting the fracture point of the load-displacement curve with the zero point. The mass-specific energy to fracture was measured as the area under the load-displacement graph prior to fracture, normalised with respect to particle mass. A Weibull distribution (Weibull modulus (m), reference stress (σ_0)) was fitted to the strength data.

The microstructure of the LWA pellets was investigated by optical microscopy (Carl Zeiss Axioscope equipped with a computer controlled stage and camera (AxioCam), with software analysis by AxioVision 4.7).

2.4. Experimental design

A statistically designed experiment following dual mixture-process response surface methodology (RSM) was followed using the Design-Expert© 8.0.2 software,[34] specialised in

design of experiments (DoE). The aim was to identify mix compositions and sintering conditions able to produce LWA pellets with specific particle density ρ_{rd} and water absorption WA_{24} with minimal variability. The dual RSM approach accounts for unknown sources of variability in the quality measures (ρ_{rd} and WA_{24}), in addition to predicting average levels, as in the simple RSM. The green LWA paste mass M_T (Eq. A2) was kept constant at 60 g for all the mix formulation ranges shown in Table 1. Additional mixture constraints are provided in Eq.A3 and A4. The exact mixture and firing temperatures of the runs are shown in the Table S2. The relative ratio of glass and clay, the two main mix ingredients, varied from 0.08 to 0.25. The suitability and adequacy of the experimental design was verified using specific DoE criteria, as defined and implemented within the Design-Expert© 8.0.2 software [34] such as: IV-optimality via maximisation of fraction of design space plots; absence of aliasing; enough degrees of freedom (d.f.) available for estimation of lack-of-fit; and no leverages at 1.

2.5. ANOVA and model fitting

Analysis of variance (ANOVA) was performed on the test results for each response variable (averages and variability). ANOVA was used to identify parametric equations that satisfactorily fit the measurements and can be used to navigate the response surface and predict the average density, water absorption and variability. The best fitting model was selected and validated by a sequence of steps, which are described in SI. Table 2 lists the statistics reported for the ANOVA models.

2.6. Simultaneous mixture composition, temperature and LWA properties optimisation

Concurrent multiple factor and response variable optima were obtained using the Design-Expert© 8.0.2, following the desirability optimisation methodology (DOM).[35, 36] Goals were

set considering the financial implications of raw materials and processing and the required specification for LWA pellets. The LWA specifications (ρ_{rd} and WA_{24}) were chosen based on: (i) the general aim to achieve minimal WA while remaining substantially lightweight; (ii) with the exact values informed by what was considered as feasible from the RSM ρ_{rd} vs WA_{24} scatterplot results (Figure 1B); along with (iii) extensive consultation with industry which indicated the ideal trade-off between WA and lightweightness. The low-cost mix components (glass, clay and water) were within ranges explored in the designed RSM experiments, while the more expensive additives (Polybor Flow® and sodium silicate) were minimised. The processing temperature was also minimised to achieve greater energy efficiency. Exact settings for the optimisation scenarios explored are shown in SI Table S3.

3. Results

3.1. Correlations: Expansion, density, water absorption, moisture, green size

Diametrical expansion, particle density and water absorption were obtained for each specific combination of mix formulations and processing conditions, as shown in SI Table S4. The experiments resulted in LWAs with a wide range of properties suitable for use in various applications.

A strong negative correlation was evident between oven-dry density of LWA pellets and diametrical expansion during rapid sintering ($R^2_{adj} = 0.91$, $P < 10^{-6}$) (Figure 1A). The 24-hour water absorption (WA_{24}) and the oven dry density (ρ_{rd}) were also negatively correlated ($R^2_{adj} = 0.58$, $P < 10^{-6}$) (Figure 1B). The WA_{24} increased as the density decreased and vice-versa. Higher WA_{24} was also associated with higher diametrical expansion and lower particle density, with these three properties being highly correlated ($R^2_{adj} = 0.87$, $P < 10^{-6}$).

3.2. Correlation between LWA properties and mixture-process factors

The firing temperature and the addition of borates are the most important factors controlling the ρ_{rd} and WA_{24}. At 750 °C almost all the pellets contracted (%ΔD_{bl} from -1.5 to -11.1), while at 900 °C most of the pellets expanded during firing. LWAs with high density and low water absorption resulted from firing at low temperatures, while the converse occurred at higher temperatures. At each temperature, the lowest density was always observed for mixes with the highest borate content (12.5% w/w). At 900 °C, samples with the minimum addition of borates (3.13% w/w) had densities as low as 1.16 $g.cm^{-3}$, which is within the desirable specification. Temperature and borate content are significant ($P < 10^{-7}$) in explaining the most of the variation in ρ_{rd}.

At 750 °C, WA_{24} is generally below 7.5% w/w_d irrespective of borate content. At 825 °C the amount of borate present seems to control WA_{24}, with high values observed for high borate contents. Firing at 900 °C results in a wider range of WA_{24} values (1.6-136.8% w/w_d), indicating that the water absorption depends increasingly on mix composition. At the highest temperature, low borate content (3.15-5.47% w/w) results in LWAs with water absorption below 49% w/w_d, while high borate (10.16-12.5% w/w) produces pellets in the range 51.8-136.8% w/w_d. Temperature and borate content are both significant ($P < 10^{-5}$), but account for only about half the variability in WA_{24} ($R^2_{adj} = 0.560$, $F_{2,52} = 35.4$).

3.3. RSM model fitting to LWA properties

Statistically significant models were fitted for all the dependent variables under examination (Table 2). These included ρ_{rd} (Figure 2A) and WA_{24} (Figure 2B). All the ANOVA underlying assumptions and model selection criteria were met. Two runs fired at relatively high temperatures of 825 °C and 900 °C showed unexpected shrinkage and these were omitted because the high leverage level could mislead model selection. A logarithmic (base10) Box-Cox transformation was applied to all properties, with the exception of ρ_{rd} (no

transformation), to best meet the ANOVA prerequisites of normality and homogeneity of variance. Thus, the predicted values refer to the median, rather than the arithmetic mean of the properties modelled.

The processing temperature is the critical factor affecting the average density of pellets as clearly illustrated by the 3D diagram of the model shown in Figure 2B. This demonstrates that the density decreases as the temperature increases. Mix components have a much less significant influence. Increasing the sodium silicate addition results in reduction in the response surface slope, resulting in higher temperatures required to achieve the lowest densities. In the region of high temperature and high borates, the model does not adequately describe the combined temperature-borate quadratic effect, suggesting that density should slightly increase with higher levels of borates, whereas the experimental results show a decrease.

3.4. Simultaneous mixture composition, temperature and LWA properties optimisation

Solutions for optimal LWA pellet production as identified by the optimisation algorithms, for eight different optimisation specification scenarios are available in the SI Table S5. Irrespective of the mixture composition, the specified ranges set for LWA particle density (0.9-1.3 $g.cm^{-3}$) and water absorption (1.5-7.5% w/w_d), result in solutions that require a firing temperature in the range 825-835 °C, and indicate that WA_{24} are achievable in the range 6.1-7.2% w/w_d with ρ_{rd} in the range 1.24-1.28 $g.cm^{-3}$. The LWA manufactured following the suggested optimal mixture composition and firing temperature had WA_{24} at 4.3 ± 2.1% w/w_d and particle density at 1.35 ± 0.10 $g.cm^{-3}$ (± denotes extended uncertainty around the average values from 10 particle replicates).

The optimisation objective function may underestimate the capability of borates to enhance bloating and thus reduce particle density. Most of the suggested optimal mixture

compositions comprise 73.6% wt. glass and 6.0% wt. clay. Sodium silicate solution appears at 2 levels (0.28% wt. and 0.59% wt.) combined with two not very dissimilar low levels of the 5 times diluted borates (3.13% wt. and 3.32% wt.). The predicted variability in density ranges from 0.01-0.04 $g.cm^{-3}$ and it is feasible to keep the variability in water absorption to below 1% w/w_d.

The 'optimal' LWA replicates showed high variability in water absorption, with WA_{24} ranging from 1.6-9.8% w/w_d and a standard deviation of 3.0% w/w_d. This variability is three times the maximum limit set during the optimisation. Similarly, the density range and standard deviation were at 1.16-1.56 $g.cm^{-3}$ and 0.14 $g.cm^{-3}$ respectively. Such variability levels are towards the middle of the range measured during the response surface experiments.

3.5. Optimal LWA pellet mineralogy, microstructure and mechanical properties

Mechanical testing of optimal pellets indicated a median indirect tensile stress (σ_{50}) of 1.77 MPa, a median secant stiffness ($K_{s,50}$) of 2463 $N.m^{-1}$, and a median mass-specific energy to fracture ($E_{m,50}$) of 27.5 $J.g^{-1}$. The tensile stress results were characterized by fitting a Weibull distribution with Weibull modulus (m) of 1.17 and reference stress (σ_0) of 3.07 MPa. Figure 3 indicates that the optimal pellets can be grouped into two categories with tensile stress behaviour corresponding to weak and strong pellets; for comparison with an indicative commercially available LWA (LYTAG 4-14) refer to the Figure S1. The microstructures of the outer surface and central inner area of optimal pellets are shown in Figure S2. A foam-like inner microstructure is evident, containing a wide range of spherical macropores distributed unevenly throughout the pellet, with a high concentration of larger pores and/or one large void in the centre. The outer skin is considerably less porous and coated with patches of calcium carbonate. The cellular glass framework shows generally a smooth surface. Outlines of pores and connections between pores have a dense and uniform

microstructure without obvious signs for cracks and spalled material. The porous morphology seems not to be weakened by irregular growth or shrinkage of crystalline phases. Qualitative XRD in Figure 4 shows the mineralogy of the raw materials, the green mix and the thermal transformations occurring during processing of the optimal LWA pellets. This confirms that the green mixture is dominated by the amorphous waste glass powder (Figure 4A), with traces of α-quartz (SiO_2) and diopside ($CaMgSi_2O_6$). Phases identified in the fireclay were kaolinite ($Al_2Si_2O_5(OH)_4$), illite ($(K,H_3O)Al_2Si_3AlO_{10}(OH)_2$), siderite ($FeCO_3$) and α-quartz ($SiO_2$).

After processing into LWA, the optimal pellet contains amorphous material, as indicated by the broad curvature above the dotted background line, and new crystalline phases (Figure 4B). As in the green pellets, α-quartz and some diopside were detected. However, new crystalline phases, α-cristobalite (SiO_2) and wollastonite ($CaSiO_3$) are formed, while mullite (Al_2SiO_5) is also possibly present, but peaks of the latter are close to detection limits and hard to distinguish from sillimanite, which however is less likely to form.

4. Discussion

The RSM methodology has been successfully applied to optimise key properties of LWAs. It has been shown that using a LWA production process involving rapid sintering at relatively low temperatures between 750-900 °C, it is feasible to produce LWA from mixes of glass-clay-sodium silicate-borate with a very wide range of densities and water absorption. Bloating, which directly results in low density, occurs for most mix compositions at 825 °C. Firing at ~825 °C produces close to optimal LWAs for a range of compositions in the glass-clay-sodium silicate-borate system. This is at least 350 °C lower than typical commercial waste-derived LWAs fired at 1400 °C[12], potentially delivering energy use, emissions and cost savings, which however have to be quantified in further studies and at pilot/full scale runs.

The wide range of density and water absorption properties achieved suggests this system can deliver products customised for a wider range of LWA applications. For example, other high value applications, such as solid media for trickling filters treating wastewater and odour treatment filters may be feasible given the high water absorption values of up to 136.8% w/w_d achieved by sintering selected formulations at higher temperatures.

There are strong interdependencies between the diametrical expansion, particle density and 24 hour water absorption. Bloating is well understood for clays[37] and recently for foamed glass.[38] Trace components are volatilised at temperatures where the glassy phase has softened. The evolved gasses are then trapped within the viscous melt and this causes expansion and the vesicular structure of inner voids, as shown in Figure S2. The fireclay used here is not anticipated to considerably contribute to the bloating as a fluxing agent, because of its high Al_2O_3 content (35.6% wt. - Table S1), which clearly classifies it well outside the range of bloating clays.[37]

The optimal compositions rapidly sintered in the temperature range 825-835 °C produces glass-clay-sodium silicate-borates LWAs with exceptionally low water absorption. Achievable water absorptions are 6.1-7.2% w/w_d (with target: 1.5-7.5% w/w_d); while remaining substantially lightweight: densities of 1.24-1.28 $g.cm^{-3}$ (target: 0.9-1.3 $g.cm^{-3}$).

Coating green pellets with calcium carbonate powder resulted in LWAs with patched surfaces due to the expansion process and the different surface texture resulting may have different properties. The mechanical properties of LWAs depend on a series of microstructural properties including density, pore size distribution, thickness of the connecting internal web, cracks/internal defects and mineralogy. The crystalline silicate phases forming during sintering do not seem to weaken the foam-like structure, and mullite and wollastonite may form elongated needle-like crystals, which embedded in glass may provide a reinforcing effect.

At each temperature the lowest density is always observed for mixes with the highest borate content, suggesting that fluxing promotes bloating, as anticipated. However, the best possible ANOVA model fitted for density (Table 2 and Figure 2A) is not sensitive to the change of borate content at low temperatures, falsely indicating the opposite effect at T = 750 °C. The model gives better fitting results as the temperature increases, but for T relevant for the optimised pellet (825-835°C) is still relatively indifferent to borate content fluctuations. This is a limitation of the model, which, however, did not prevent from identifying a verified composition and process conditions for the optimal LWA. However, it suggests that further optimisation towards minimising the use of borates could be potentially feasible by running new RSM experiments narrowed down around the identified optimised area.

Mineralogical transformations occur during sintering that maintain the dominant amorphous glassy phase, while new crystalline phases form, transforming the initial raw materials into a new ceramic/glass composite microstructure. During rapid sintering at temperatures around 825 °C new crystalline phases are formed that were not present in the green LWA pellets. Kaolinite and illite are not detected in fired LWA pellets because they decompose. Kaolinite thermally decomposes by dehydroxylation at 500-600 °C to poorly crystalline metakaolin. Crystallization of spinel phases should only begin at temperatures above 900 °C.[39] Illite dehydroxylates between 350 and 600 °C, and cannot be detected by XRD in samples fired above 700 °C. At 825 °C illite is expected to break down (700-850 °C) and it has been observed that above the dehydroxylation temperatures, Si-rich liquid phases form from kaolinite and illite which cannot crystallise into spinel. Diopside is stable at these firing temperatures and is detected in the final product. Wollastonite is a common phase in Ca-bearing silicate glasses: for example, it has been observed at 775ºC using basic oxygen furnace slags as starting material.[40] Wollastonite formation has been reported during firing at 825 °C for 1 hour of compositions containing $CaO–MgO–Na_2O–P_2O_5–SiO_2–CaF_2$.[41]

Cristobalite is a polymorph of silica, which is only stable above 1470 °C, the equilibrium formation temperature, but this can form from quartz, as β-cristobalite above 227 °C. Cristobalite has been found to precipitate when an initially amorphous borosilicate glass was sintered, with devitrification occurring between 700-1000 °C.[42] During cooling both quartz and cristobalite undergo phase transitions to their low-temperatur polymorphs (α-quartz <573º and α-cristobalite <227ºC). Both phase transition are accompanied with volume contraction which could have a potentially weakening effect on the cellular structure of the pellets. However, cracks due to shrinkage were not observed (Figure S2) indicating that the low proportion of both silica phases compared to the glass phase resulted only in negligible destabilizing effects on the pellet microstructure.

In these experiments the glass is predominantly soda-lime-silica. Boron was not detected in any crystalline phases and B_2O_3 is likely to be incorporated in the glassy phase, serving as a network former. It is proposed that Al from kaolinite and illite combine with the Si available from the amorphous waste glass, liquid sodium silicate, kaolinite and illite to form mullite. No iron containing crystalline phases were detected in the fired LWA pellets. Siderite thermally decomposes between 500-600 °C [43] by decomposition/decarbonation with the resultant phases formed depending on the exact firing conditions.[44]

The mineralogy is also a factor potentially affecting LWA particle density because of the varying density of the different crystalline phases. However, both green and sintered LWAs are dominated by the amorphous glassy phase rather than the crystalline phases. Therefore little differentiation could be anticipated due to mineralogy, and this should relate to the variable amount of glass present in the green mix. However, the glass content, while statistically significant (Table 1 - mixture component A), was not found to been as important predictive factor for particle density as temperature: it could be speculated that there is possibly sufficient quantity of glass in each mixture formulation for purposes related to

bloating, and therefore particle density, varying only within a relatively narrow range (64-74% wt.).

Discrete sets of weak and strong LWA pellets were evident. The strong sub-group had tensile strengths between 1.5-8.0 MPa and this suggests a variable microstructure between individual LWA pellets. Reducing the average particle size of the LWAs is expected to result in higher tensile strength values. Forming the green pellets mechanical by standardised pelletisation could potentially reduce variability. It is has to be explored whether mechanised formation could limit or eliminate the existence of weaker pellets, which may have been overly compressed, resulting in the introduction of undesirable cracks, carried over during sintering.

Artificial LWAs can be engineered to a defined specification by using a combined mixture-process dual RSM, applied with desirability multi-objective optimisation. This develops empirical models capable of predicting optimum average target values for LWA properties. Overall, the optimal LWA produced using the RSM is a novel product with exceptionally low water absorption and appropriate density. This outcome has significant sustainability credentials as it incorporates a very high percentage of widely available and currently not recycled waste glass. It is produced by rapid firing at low temperature, potentially preserving energy and lowering carbon emissions. Optimisation goals met, included the financial implications of raw materials. These features make this product attractive for a range of applications, and particularly for structural LWAC. Pilot and full scale tests are needed to verify the commercial viability of the glass upcycling technology which was developed and tested here on lab scale. Despite extensive use of commercially produced glass aggregate in concrete, concern over the potential for alkali silica reaction (ASR) remains and further research work is needed to investigate this effect for the LWA produced here. In the next phase of R&D further recovering of waste resources and reduction

of manufacturing costs could be explored by potentially replacing the chemical grade additives (sodium silicate and Polybor Flow®) with waste-derived substitutes.

Acknowledgements

This research received financial support from the Technology Strategy Board (TSB) project "Sustainable Innovative Lightweight Expanded Clay-Glass (SILEC-G)" (Project No. AB267G). We gratefully acknowledge the input of the industrial partners, including Mike Evans and Bert Bingham of Claylite Aggregates Limited, and Hugh Bowerman, Alan Cooper and John Moran of Laing O'Rourke. We are grateful to Wayne Adams of Stat-Ease for support with developing and applying the statistical experimental design. We also thank David Lever of Rio Tinto Minerals for insights on the use of borates. Peter Roche Vaughan, Hara Spathi, Clive Galea and Tassos Kampaksis have assisted with the laboratory preparation and testing of LWA. The opinions expressed herein are those of the authors' alone.

Supporting Information Available

It includes details of: (i) ANOVA and model selection procedure; (ii) chemical composition, moisture and loss on ignition of the solid mixture components; (iii) experimental runs (mixture formulations and firing temperatures) and detailed results; (iv) RSM optimisation scenarios settings and solutions; (v) compressive stress performance of a standard commercial LWA (LYTAG 4-14); and (vi) microstructure of the optimal pellet. This information is available free of charge via the internet at: http://pubs.acs.org/.

Appendix

$$\%\Delta D_{bl} = \frac{D_f - D_i}{D_i} \times 100$$ [**Eq. A1**]

$$M_{tw} = M_g + M_c + M_w + M_{ss} + M_b$$ [**Eq. A2**]

$$0.08 \leq \frac{M_c}{M_g} \leq 0.25$$ [**Eq. A3**]

$$M_w = M_{tw} + M_{ssw} + M_{bw} = \frac{1}{4}\left(M_g + M_c\right)$$ [**Eq. A4**]

References

1. Wise, C.; Pawlyn, M.; Braungart, M., Eco-engineering: Living in a materials world. *Nature* **2013,** *494*, (7436), 172-175.
2. Tonini, D.; Martinez-Sanchez, V.; Astrup, T. F., Material Resources, Energy, and Nutrient Recovery from Waste: Are Waste Refineries the Solution for the Future? *Environ. Sci. Technol.* **2013,** *47*, (15), 8962-8969.
3. Kenny, S. T.; Runic, J. N.; Kaminsky, W.; Woods, T.; Babu, R. P.; Keely, C. M.; Blau, W.; O'Connor, K. E., Up-Cycling of PET (Polyethylene Terephthalate) to the Biodegradable Plastic PHA (Polyhydroxyalkanoate). *Environ. Sci. Technol.* **2008,** *42*, (20), 7696-7701.
4. Wang, S.; Xing, J.; Jang, C.; Zhu, Y.; Fu, J. S.; Hao, J., Impact Assessment of Ammonia Emissions on Inorganic Aerosols in East China Using Response Surface Modeling Technique. *Environ. Sci. Technol.* **2011,** *45*, (21), 9293-9300.
5. Ahmad, A. L.; Ismail, S.; Bhatia, S., Optimization of Coagulation−Flocculation Process for Palm Oil Mill Effluent Using Response Surface Methodology. *Environ. Sci. Technol.* **2005,** *39*, (8), 2828-2834.
6. Capon, D., Recycling using glass cullet. *Glass International* **2013,** *36*, (7), 32-33.
7. Tsai, C. L.; Krogmann, U., Material Flows and Energy Analysis of Glass Containers Discarded in New Jersey, USA. *Journal of Industrial Ecology* **2013,** *17*, (1), 129-142.
8. Velis, C. A.; Wagland, S.; Longhurst, P.; Robson, B.; Sinfield, K.; Wise, S.; Pollard, S., Solid recovered fuel: Materials flow analysis and fuel property development during the mechanical processing of biodried waste. *Environ. Sci. Technol.* **2013,** *47*, (6), 2957-2965.
9. Larsen, A. W.; Merrild, H.; Christensen, T. H., Recycling of glass: Accounting of greenhouse gases and global warming contributions. *Waste Manage. Res.* **2009,** *27*, (8), 754-762.
10. British Glass Manufacturers' Confederation *UK glass manufacture: 2008 - a mass balance*; British Glass Manufacturer's Confederation: London, 2009.
11. Coleman, N. J.; Li, Q.; Raza, A., Synthesis, structure and performance of calcium silicate ion exchangers from recycled container glass. *Physicochemical Problems of Mineral Processing* **2014,** *50*, (1), 5-16.
12. Ahmad, S.; Sallam, Y. S.; Al-Hashmi, I. A. R., Optimising dosage of Lytag used as coarse aggregate in lightweight aggregate concretes. *Journal of the South African Institution of Civil Engineering* **2013,** *55*, (1), 80-84.
13. Chandra, S.; Berntsson, L., *Lightweight aggregate concrete: science, technology, and applications*. Noyes Publications: New York, USA, 2003; p 430.
14. De'Gennaro, R.; Graziano, S. F.; Cappelletti, P.; Colella, A.; Dondi, M.; Langella, A.; De'Gennaro, M., Structural concretes with waste-based lightweight aggregates: From landfill to engineered materials. *Environ. Sci. Technol.* **2009,** *43*, (18), 7123-7129.
15. Ducman, V.; Mirtic, B., The applicability of different waste materials for the production of lightweight aggregates. *Waste Manage.* **2009,** *29*, (8), 2361-2368.
16. Cheeseman, C. R.; Virdi, G. S., Properties and microstructure of lightweight aggregate produced from sintered sewage sludge ash. *Resour. Conserv. Recy.* **2005,** *45*, (1), 18-30.
17. Cheeseman, C. R.; Makinde, A.; Bethanis, S., Properties of lightweight aggregate produced by rapid sintering of incinerator bottom ash. *Resour. Conserv. Recy.* **2005,** *43*, (2), 147-162.
18. Dong, S. H.; Ge, Y.; Zhang, B. S.; Yuan, J., Effect of Lightweight Aggregate Moisture Content on Pore Structure of Concrete. In *Advances in Building Materials, Pts 1-3*, Li, L. J., Ed. Trans Tech Publications Ltd: Stafa-Zurich, 2011; Vol. 168-170, pp 647-651.
19. Newman, J. B., Properties of structural lightweight aggregate concrete. In *Structural lightweight aggregate concrete*, Clarke, J. L., Ed. Chapman & Hall: UK, 1993; pp 19-41.
20. Liles, K. J.; Tyrrell, M. E. *Waste glass as a raw material for lightweight aggregate*; US Goveernment printing office: 1975-603-775/59; U.S. Bureau of Mines - University of Alabama: 1976; p 8.

21. Ducman, V.; Mladenovic, A.; Suput, J. S., Lightweight aggregate based on waste glass and its alkali-silica reactivity. *Cem. Concr. Res.* **2002,** *32*, (2), 223-226.
22. Kourti, I.; Cheeseman, C. R., Properties and microstructure of lightweight aggregate produced from lignite coal fly ash and recycled glass. *Resour. Conserv. Recy.* **2010,** *54*, (11), 769-775.
23. Mun, K. J., Development and tests of lightweight aggregate using sewage sludge for nonstructural concrete. *Constr. Build. Mater.* **2007,** *21*, (7), 1583-1588.
24. Nemes, R.; Jozsa, Z., Strength of lightweight glass aggregate concrete. *J. Mater. Civ. Eng.* **2006,** *18*, (5), 710-714.
25. Uwe, E. A.; Boccaccini, A. R.; Cook, S. G.; Cheeseman, C. R., Effect of borate addition on the sintered properties of pulverised fuel ash. *Ceram. Int.* **2007,** *33*, (6), 993-999.
26. Lever, D., Increase capacity without capital investment: the use of borate to increase kiln throuhput at a brick plant. *Inerceram* **2004,** *53*, (3), 174-176.
27. Chen, B.; Wang, K.; Chen, X.; Lu, A., Study of foam glass with high content of fly ash using calcium carbonate as foaming agent. *Mater. Lett.* **2012,** *79*, 263-265.
28. Vining, G. G.; Myers, R. H., Combining Taguchi and response-surface philosophies - a dual response approach. *J. Qual. Technol.* **1990,** *22*, (1), 38-45.
29. Harrington, E. C. J., The desirability function. *Industrial Quality Control* **1965,** *21*, (10), 494-498.
30. British Standards, BS EN 1097-6:2000. Tests for mechanical and physical properties of aggregates - Part 6: Determination of particle density and water absorption. Incorporating Corrigendum No. 1 and Amendment No. 1. In BSI: 2000; p 32.
31. British Standards, BS EN ISO 10545-3:1997. Ceramic tiles. Determination of water absorption, apparent porosity, apparent relative density and bulk density. In British Standards: 1997; p 12.
32. Hiramatsu, Y.; Oka, Y., Determination of the tensile strength of rock by a compression test of an irregular test piece. *Int. J. Rock Mech. Min.* **1966,** *3*, (2), 89-90.
33. Cavarretta, I.; Coop, M.; O'Sullivan, C., The influence of particle characteristics on the behaviour of coarse grained soils. *Geotechnique* **2010,** *60*, (6), 413-423.
34. Stat-Ease *Design-Expert 8. Software for design of experiments (DOE)* Version 8.0.2: 2011.
35. Derringer, G.; Suich, R., Simultaneous-optimization of several response variables *J. Qual. Technol.* **1980,** *12*, (4), 214-219.
36. Castillo, E. D.; D.C., M.; McCarville, D. R., Modified desirability functions for for multiple response optimization. *J. Qual. Technol.* **1996,** *12*, (4), 337-344.
37. Riley, C. M., Relation of chemical properties to the bloating of clays. *J. Am. Ceram. Soc.* **1950,** *34*, (4), 121-128.
38. Steiner, A. C. Foam glass production form vitrifield municipal waste ashes. Technical University of Eindhoven, Düsseldorf, Germany, 2006.
39. McConville, C. J.; Lee, W. E., Microstructural development on firing illite and smectite clays compared with that in kaolinite. *J. Am. Ceram. Soc.* **2005,** *88*, (8), 2267-2276.
40. Ferreira, E. B.; Zanotto, E. D.; Scudeller, L. A. M., Glass and glass-ceramic from basic oxygen furnace (BOF) slag. *Glass Sci. Technol.* **2002,** *75*, (2), 75-86.
41. Kansal, I.; Tulyaganov, D. U.; Goel, A.; Pascual, M. J.; Ferreira, J. M. F., Structural analysis and thermal behavior of diopside–fluorapatite–wollastonite-based glasses and glass–ceramics. *Acta Biomater.* **2010,** *6*, (11), 4380-4388.
42. Jean, J. H.; Gupta, T. K., Cristobalite growth inhibitor in pyrex borosilicate glass gallium oxide. *J. Mater. Res.* **1993,** *8*, (8), 1767-1769.
43. Gallagher, P. K.; Warne, S. S. J., Thermomagnetometry and thermal decomposition of siderite. *Thermochim. Acta* **1981,** *43*, (3), 253-267.
44. Koziol, A. M., Experimental determination of siderite stability and application to Martian Meteorite ALH84001. *Am. Mineral.* **2004,** *89*, (2-3), 294-300

Table 1. Range of values set for the LWA mixture paste formulations and processing factors.

Mix component		**Mass**[†] **(g)**		**Percentage (wt.%)**	
	Symbol	Min	Max	Min	Max
Glass	g	38.4	44.2	63.9	73.6
Clay	c	3.5	9.6	5.9	16.0
Water[*]	w	4.1	10.1	6.8	16.9
Sodium silicate[***]	ss	0.16	1.15	0.27	1.91
Borate[**]	b	1.88	7.50	3.13	12.51
Firing temperature	T	750 °C	900 °C		

[*] Additional tap water ($\%M_{TW}$)
[**] Sodium silicate solution ($\%M_S$) and diluted Polybor® Flow ($\%M_B$), including water content
[***] Sodium silicate specific gravity = 1.375, resulting in 0.25-1.75% vol.
[†] Out of a total of 60 g

Table 2. ANOVA for best fitting regression models selected for navigating the design space and predicting responses for average (av) measure as arithmetic mean and variability, measured as standard deviation (sd) of the particle density (ρ_{rd}) and 24 hour water absorption (WA_{24}).

Statistics	av(ρ_{rd})	sd(ρ_{rd})	av(WA_{24})	sd(WA_{24})
Regression model	Reduced Quadratic × Quadratic	Reduced Cubic × Mean	Reduced Quadratic × Linear	(Reduced Linear + Squared) × Quadratic
Box-Cox transformation	None	Log (base 10)	Log (base 10)	Log (base 10)
λ	1	0	0	0
SSR	1.14	0.66	15.71	14.52
d.f. (Residual)	42	21	42	46
MSR	0.027	0.031	1.31	1.82
SSE	13.45	3.97	2.35	4.97
d.f. (Model)	12	32	12	8
MSE	1.12	0.12	0.056	0.11
F value (Model)	41.21	3.97	23.38	16.81
P value (Model) (Prob > *F*)	<0.0001	0.0008	<0.0001	<0.0001
R^2_{adj}	0.90	0.64	0.83	0.70
R^2_{pred}	0.85	0.25	0.76	0.64
$R^2_{adj} - R^2_{pred}$	0.05	0.4	0.08	0.06
F Lack-of-fit (LoF)	6.22	0.48	5.88	1.05
d.f. (LoF)	37	16	37	41
P (LoF)	0.025	0.88	1.10	0.54
LoF significant	Yes	No	No	No
MS (Pure error)	0.0049	0.26	0.26	0.10
d.f. (Pure error)	5	5	5	5
Adequate model precision	22.9	7.4	17.9	15.5
Model term	A, B, C, D, E, **AF, BC, **BF, **CE, **CF, **EF, **CEF, EF^2	A, B, C, D, E, **AB, AC, AE, **BC, BD, BE, **CD, CE, **DE, ABC, ABD, ABE, ACD, ACE, ADE, BCD, BCE, BDE, CDE, AC(A-C), AD(A-D), AE(A-E), BC(B-C), BD(B-D), BE(B-E) CD(C-D), CE(C-E)	A, B, C, D, E, AC, **AF, CD, **CF, **DF, EF, **ACF, CDF	A, B, C, D, E, CF, **EF, CF^2, **EF^2

* Typical DoE nomenclature followed. See Table S2 for model term (A to E) definitions. SSR: regression sum of squares; d.f.: degrees of freedom used for model evaluation; MSR: regression mean of squares; SSE: error sum of squares: MSE: error mean square; R^2_{adj}: adjusted coefficient of multiple determination; R^2_{pred}: predicted coefficient of multiple determination. The first term of the regression models products refers to the mixture and the second to the process (firing temperature).

** Model terms not statistically significant (α = 0.05), but included to respect hierarchy

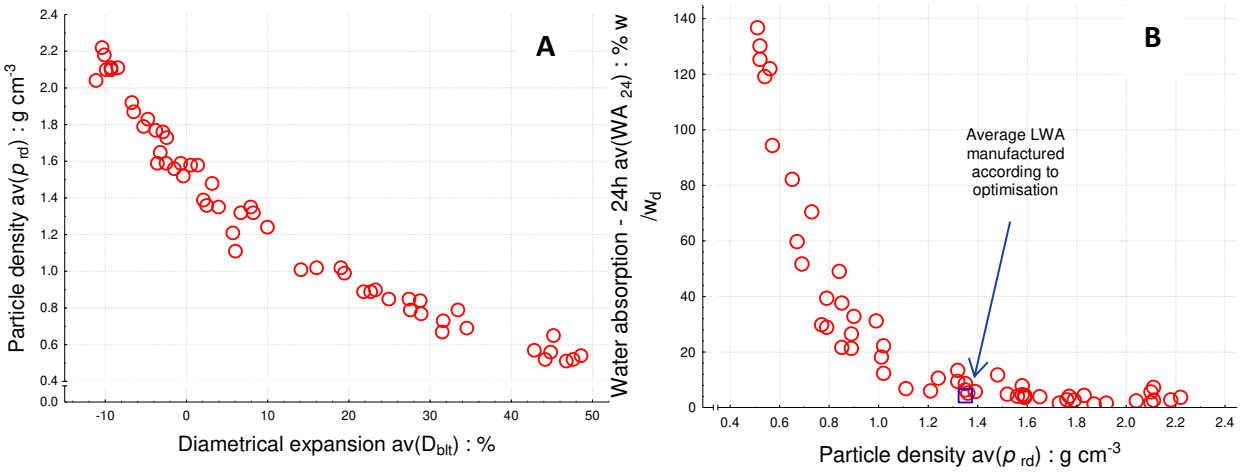

Figure 1. (A) Average particle dry density against average diametrical expansion; and (B) 24-h water absorption against average particle dry density, for the LWA pellets manufactured in line with the DoE experimental runs. Strong correlations are evident for both (A) and (B). The different colour squared data point in (B) indicates the actual average LWA that has resulted from the optimisation.

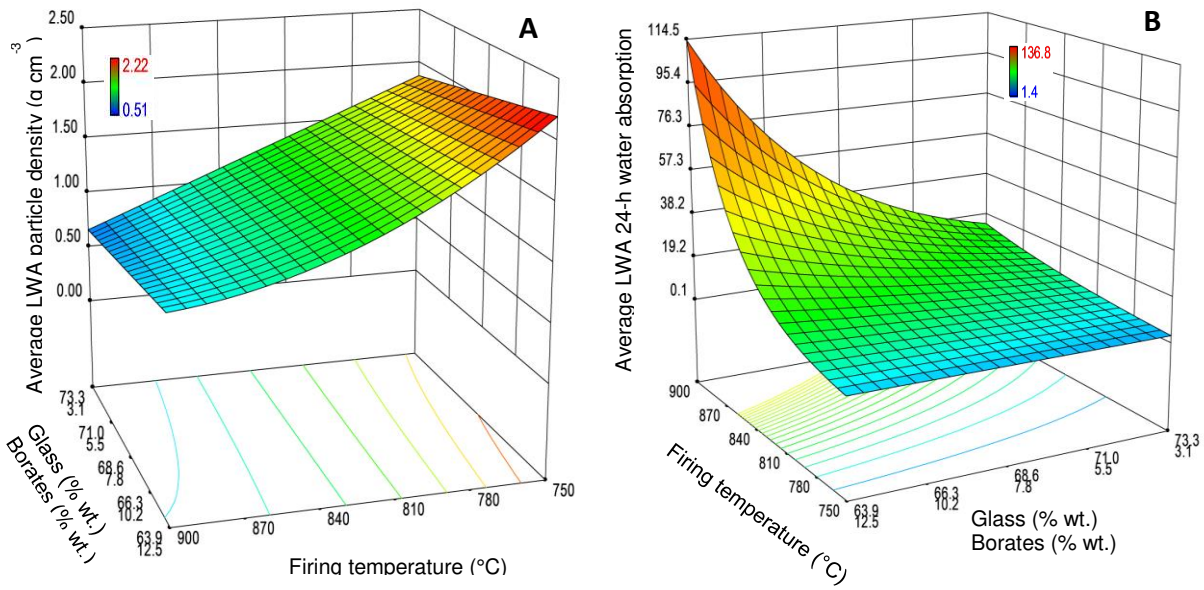

Figure 2. 3-dimensional grid and 2-dimensional contour plots of model fitted for average: (A) particle density and (B) 24-hour water absorption of LWA pellets. Plotted for middle levels of clay (10.5% wt.), sodium silicate (1.06% wt.) and added water (11.9% wt.).

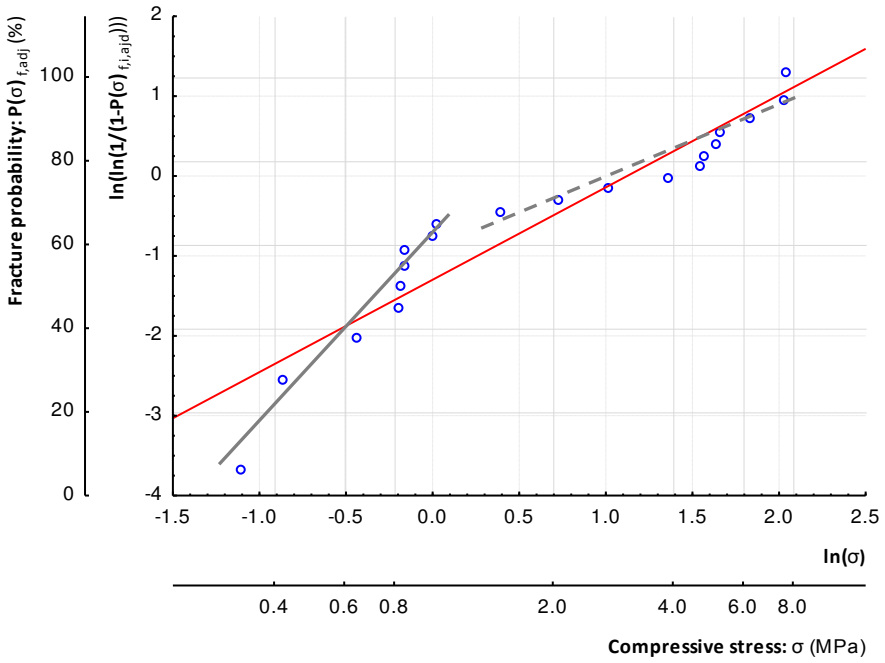

Figure 3. Compressive stress performance of LWA pellets. A Weibull distribution curve fit to the 20 samples of optimised LWA pellets (NCO: $\ln(\ln(1/(1-P(s)_{f,i,ajd}))) = -1.30 + 1.16 * \ln(\sigma)$). The optimal glass-clay-borates LWA fit is not ideal, because 2 different sub-groups of pellets regarding tensile stress are evident ('weak': solid grey line, and 'strong': dotted grey line). For comparison with a standard commercial LWA (LYTAG 4-14) (LYTAG: $\ln(\ln(1/(1-P(\sigma)_{f,i,adj}))) = -4.26 + 3.39 * \ln(\sigma)$) refer to the Supporting Information Figure SI1.

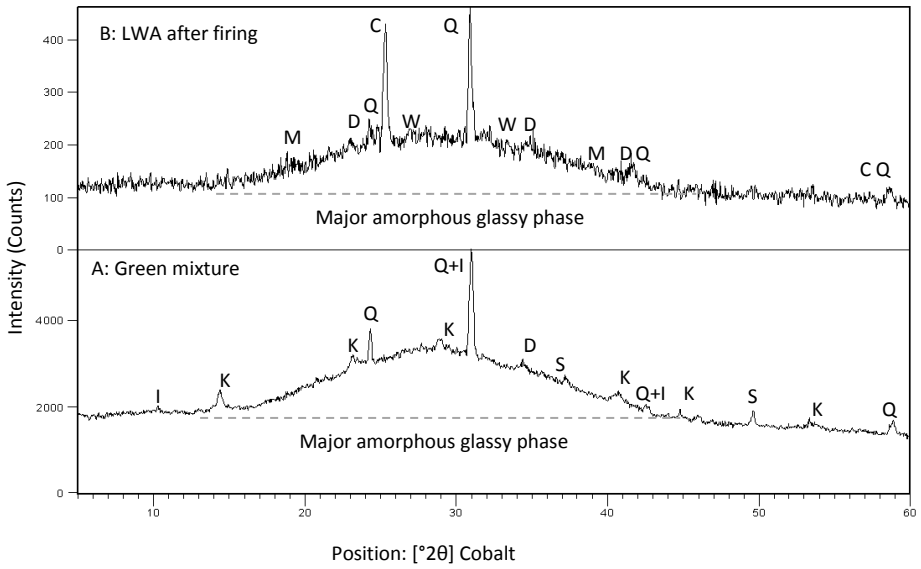

Figure 4. Mineralogy (X-ray diffractogram) of: (A) green mixture of raw material; and (B) of the optimal LWA pellet after firing. Crystalline phases key: C: cristobalite; D: diopside; Q: a-quartz; I: illite; K: kaolinite; M: mullite; S: siderite; W: wollastonite.